Analytical Performance of Polymer-Based Microfluidic Devices Fabricated By Computer Numerical Controlled Machining

ARTICLE *in* ANALYTICAL CHEMISTRY · MARCH 2006

Impact Factor: 5.64 · DOI: 10.1021/ac051523y · Source: PubMed

8 AUTHORS, INCLUDING:

Ken Wehmeyer
Procter & Gamble
68 PUBLICATIONS **1,226** CITATIONS

SEE PROFILE

Anal. Chem. **2006,** *78,* 936−941

Analytical Performance of Polymer-Based Microfluidic Devices Fabricated By Computer Numerical Controlled Machining

Justin S. Mecomber,† Apryll M. Stalcup,† Doug Hurd,‡ H. Brian Halsall,† William R. Heineman,† Carl J. Seliskar,† Kenneth R. Wehmeyer,§ and Patrick A. Limbach*,†

Department of Chemistry, P.O. Box 210172, and Department of Mechanical, Industrial, and Nuclear Engineering, P.O. Box 210072, University of Cincinnati, Cincinnati, Ohio 45221-0072, and Procter and Gamble Pharmaceuticals, 8700 Mason-Montgomery Road, Mason, Ohio 45040

A study comparing the electrophoretic separation performance attainable from microchips molded by masters fabricated using conventional CNC machining techniques with commercial microchips, wire imprinted microchips, and microchips from LIGA molding devices is presented. An electrophoresis-based detection system using fluorescence microscopy was used to determine the analytical utility of these microchips. The separation performance of CNC microchips was comparable to commercially available microchips as well as those fabricated from LIGA masters. The important feature of the CNC machined masters is that they have rapid design-to-device times using routinely available machining tools. This low-cost prototyping approach provides a new entry point for researchers interested in thermoplastic microchips and can accelerate the development of polymer-based lab-on-a-chip devices.

Microfabricated devices have been developed for various analytical uses such as detecting small organic ions,[1] chemical warfare agents,[2] and heavy metal analysis.[3] They have accelerated progress in DNA separations,[4−6] proteomics,[7,8] and carbohydrate analysis[9] and have been used in applications such as drug delivery and discovery,[10,11] clinical analysis,[12] immunoassays,[13] and bioaffinity interactions.[14] Although there are many applications for these devices, there are concerns related to their cost, availability, and fabrication. Recently, there has been interest in comparing the performance characteristics of glass- and polymer-based devices,[15] since the latter have the advantages of disposability, higher possible aspect ratios, and can be fabricated by an assortment of less expensive techniques.[16]

Polymer microchip devices can be generated by a variety of methods. Compression molding techniques, such as hot embossing[17−19] and injection molding,[20−22] permit rapid and accurate replication. While the molding master is fundamental to these types of fabrication, they can be expensive to make. Recently, ways to fabricate prototype molding masters economically have been developed. Some of the manufacturing methods used to prototype molding tools include UV-photoablation,[23] microthermoforming,[24] computer numerical controlled (CNC) milling,[25] and improved masking technologies.[26−30]

* To whom correspondence should be addressed. Phone (513) 556-1871. Fax (513) 556-9239. E-mail: Pat.Limbach@uc.edu.

† Department of Chemistry, University of Cincinnati.

‡ Department of Mechanical, Industrial, and Nuclear Engineering, University of Cincinnati.

§ Procter and Gamble Pharmaceuticals.

(1) Willauer, H. D.; Collins, G. E. *Electrophoresis* **2003**, *24*, 2193−2207.
(2) Wang, J. *Anal. Chim. Acta* **2004**, *507*, 3−10.
(3) Tokeshi, M.; Kikutani, Y.; Hibara, A.; Sato, K.; Hisamoto, H.; Kitamori, T. *Electrophoresis* **2003**, *24*, 3583−3594.
(4) Zhang, L.; Dang, F.; Baba, Y. *J. Pharm. Biomed. Anal*. **2003**, *30*, 1645−1654.
(5) Kricka, L. J.; Wilding, P. *Anal. Bioanal. Chem.* **2003**, *377*, 820−825.
(6) Kolchinsky, A. M.; Gryadunov, D. A.; Lysov, Y. P.; Mikhailovich, V. M.; Nasedkina, T. V.; Turygin, A. Y.; Rubina, A. Y.; Barsky, V. E.; Zasedatelev, A. S. *Mol. Biol.* **2004**, *38*, 4−13.
(7) Lacher, N. A.; Garrison, K. E.; Martin, R. S.; Lunte, S. M. *Electrophoresis* **2001**, *22*, 2526−2536.
(8) Lion, N.; Rohner, T. C.; Dayon, L.; Arnaud, I. L.; Damoc, E.; Youhnovski, N.; Wu, Z. Y.; Roussel, C.; Josserand, J.; Jensen, H.; Rossier, J.; Przybylski, M.; Girault, H. H. *Electrophoresis* **2003**, *24*, 3533−3562.
(9) Suzuki, S.; Honda, S. *Electrophoresis* **2003**, *24*, 3577−3582.
(10) Razzacki, S. Z.; Thwar, P. K.; Yang, M.; Ugaz, V. M.; Burns, M. A. *Adv. Drug Delivery Rev.* **2004**, *56*, 185−198.
(11) Sundberg, S. A.; Chow, A.; Nikiforov, T.; Wada, H. G. *Drug Discovery Today* **2000**, *12*, 92−103.
(12) Verpoorte, E. *Electrophoresis* **2002**, *23*, 677−712.
(13) Schmalzing, D.; Buonocore, S.; Piggee, C. *Electrophoresis* **2000**, *21*, 3919−3930.
(14) Guijt, R. M.; Baltussen, E.; Van Dedem, G. K. *Electrophoresis* **2002**, *23*, 823−835.
(15) Lacher, N. A.; de Rooij, N. F.; Verpoorte, E.; Lunte, S. M. *J. Chromatogr., A* **2003**, *1004*, 225−235.
(16) Manz, A.; Becker, H. *Microsystem Technology in Chemistry and Life Sciences*; Springer Verlag: Berlin, 1999.
(17) Becker, H.; Heim, U. *Sens. Actuators* **2000**, *83*, 130−135.
(18) Kricka, L. J.; Fortina, P.; Panaro, N. J.; Wilding, P.; Alonso-Amigo, G.; Becker, H. *Labchip* **2002**, *2*, 1−4.
(19) Heckele, M.; Bacher, W.; Muller, K. D. *Microsyst. Technol.* **1998**, *4*, 122−124.
(20) Ruprecht, R.; Benzler, T.; Hanemann, T.; Muller, K.; Konys, J.; Piotter, V.; Schanz, G.; Schmidt, L.; Thies, A.; Wollmer, H.; Haubelt, J. *Microsyst. Technol.* **1997**, *4*, 28−31.
(21) Piotter, V.; Hanemann, T.; Ruprecht, R.; Haubelt, J. *Microsyst. Technol.* **1997**, *3*, 129−133.
(22) McCormick, R. M.; Nelson, R. J.; Alonso-Amigo, G.; Benvegnu, D. G.; Hopper, H. H. *Anal. Chem.* **1997**, *1997*, 22626−2630.
(23) Rossier, J.; Reymond, F.; Michel, P. E. *Electrophoresis* **2002**, *23*, 858−867.
(24) Truckenmuller, R.; Rummler, Z.; Schaller, T. *J. Micromech. Microeng.* **2002**, *12*, 375−379.
(25) Mecomber, J. S.; Hurd, D.; Limbach, P. A. *Int. J. Machine Tools Manu.* **2005**, *45*, 1542−1550.
(26) Tan, A.; Rodgers, K.; Murrihy, J. P.; O'Mathuna, C.; Glennon, J. D. *Lab Chip* **2001**, *1*, 7−9.
(27) Manica, D. P.; Ewing, A. G. *Electrophoresis* **2002**, *23*, 3735−3743.
(28) Fiorini, G. S.; Jeffries, G. D.; Lim, D. S.; Kuyper, C. L.; Chiu, D. T. *Lab Chip* **2003**, *3*, 158−163.
(29) Narasimhan, J.; Papautsky, I. *J. Micromech. Microeng.* **2004**, *14*, 96−103.
(30) Lucio do Lago, C.; Torres Da Silva, H. D.; Neves, C. A.; Alves Brito-Neto, J. G. *Anal. Chem.* **2003**, *75*, 3853−3858.

10.1021/ac051523y CCC: $33.50
Published on Web 12/24/2005

It was previously thought that conventional CNC milling could not be used to develop prototypes and that ultraprecision milling was the only way to achieve the dimensions required for microfluidic devices.[31] While ultraprecision milling machines can fabricate the high aspect ratio structures,[32−34] they are not as readily available as CNC milling machines. Thus, we have been investigating conventional CNC milling to fabricate prototype molding masters because such mills are accessible in most commercial and university machine shops.[25] Here, conventional CNC machining is found suitable for generating molding masters that can then be used to fabricate working microfluidic devices. Analytical performance studies of simple cross-injector designs find polymer microchips made this way to be comparable to LIGA (Lithographie-Galvanoformung-Abformung) generated and commercial polymer devices as well as commercial glass-based microchips.

MATERIALS AND METHODS

Microfluidic Devices. CNC-machined molding masters and functional poly(methyl methacrylate) (PMMA; Goodfellow, Berwyn, PA) microchips were fabricated by methods previously reported.[25] Briefly, end milling using 51-μm-radii tools was used to remove aluminum from the top of the master to leave the desired positive relief structure for molding. To achieve tolerances that had been previously deemed unattainable for microchip master fabrication via CNC machining, we developed a novel alignment technique enabled by a standard microscope attached to the end mill. The site at the capillary interface was sealed by placing high-strength epoxy (Devcon, McMaster Carr, Cleveland, OH) at the end of the chip and allowing it to travel to the buffer waste reservoir by capillary action. On all microchips, additional plastic reservoirs for analyte and buffer loading were made from pipet tips and glued using high-strength epoxy. The additional volume (200 μL) of the plastic reservoirs increased reproducibility by reducing the depletion of electrolyte buffer and increasing the loading precision by minimizing siphoning effects.[35]

Other microchips compared with CNC milled microchips included commercial microchips, microchips produced from a nickel LIGA mold (Mezzo Corp., Baton Rouge, LA), and in-house-generated wire-imprinted microchips. Commercial microchips investigated included Schott Borofloat glass (Micralyne, Alberta, Canada) and PMMA multilane (Aclara, Mountain View, CA). Microchips were generated from the nickel LIGA mold via hot embossing. Wire imprinting used a previously described method[36] with slight modifications. Briefly, two pieces of copper wire of 75-μm diameter (McMaster Carr) were cut to approximately 90- and 9.5-mm lengths and straightened using two blocks of aluminum. The two pieces of thermoplastic (101.6 mm (length) × 101.6 mm (width) × 2.5 mm (thickness) (McMaster Carr)) were laid down separately on top of a high-temperature glass slide. After hot embossing, the chips were bonded to form a conventional cross microchip.

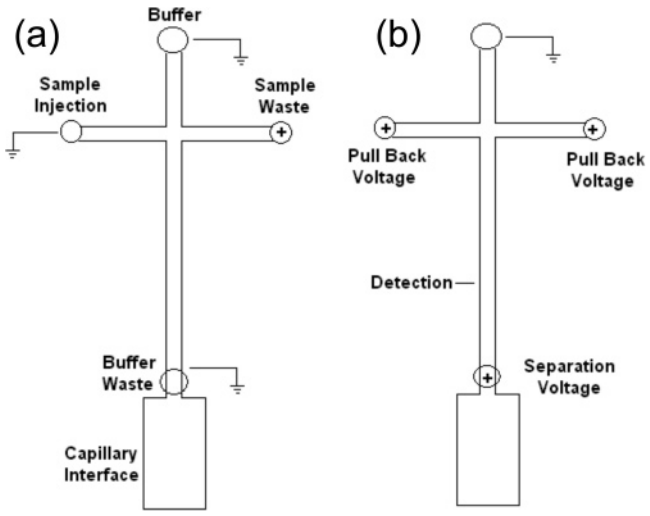

Figure 1. Design of the conventional cross injector geometry for the CNC microfluidic chips used for these experiments. A pinched injection scheme was used comprising (a) analyte loading, followed by pullback and separation voltages (b) for analyte injection and separation. The arrow symbol is used for ground, and the + represents a positive applied voltage.

Imaging. Electron microscope images were taken using a XL30 environmental scanning electron microscope (FEI Company, Hillsboro, OR). Optical images were taken using an Eastman MDS 100 digital camera (Kodak Digital Science, Rochester, NY) outfitted with a macro 10× lens (Computar).

On-Chip Electrophoresis. All on-chip electrophoresis detection experiments used a custom-built apparatus that has been described in detail previously.[37] The only modification done to the above system was to use current monitoring electronics to aid in troubleshooting. A stock buffer of 10× TBE (890 mM Tris/890 mM borate/20 mM EDTA electrophoresis grade, pH 8.4)/5% poly(ethylene oxide) (PEO) was prepared. The running buffer was made in 0.1× TBE/0.05% PEO buffer prior to use by a 100-fold dilution with distilled−deionized water. The electroosmotic modifier, PEO, was present in the buffer to allow reverse-polarity electrophoresis to be used, and to effectively coat all channel surfaces so that the viscosity was high, and surface charge was low enough that EOF would be negligible in all microchips. Stock solutions of 1 mM fluorescein isothiocyanate (FITC; Sigma, St. Louis, MO) and fluorescein (F) (Molecular Probes, Eugene, OR) were prepared in 50% aqueous methanol (Fisher, Fairlawn, NJ). Appropriate dilutions were made in 0.1 × TBE/0.5% PEO running buffer prior to use. Analyte solutions were made to 25 μM fluorescein and 50 μM fluorescein isothiocyanate for all experiments. All reagents were prepared with distilled−deionized water from a Milli-Q System (Millipore Corp., Bedford, MA) and degassed daily. Degradation of FITC was noted after 24 h.[38]

The run buffer was added to reservoirs labeled sample waste, sample injection, and buffer (Figure 1). The microchip was conditioned offline by applying a vacuum for 5 min to the buffer waste before adding the mixture to the sample reservoir. Platinum

(31) Madou, M. J. *Fundamentals of Microfabrication*, 2nd ed.; CRC Press LLC: Boca Raton, FL, 2002.
(32) Zhao, D. S.; Roy, B.; McCormick, M. T.; Kuhr, W. G.; Brazill, S. A. *Lab Chip* **2003**, *3*, 93−99.
(33) Gerlach, A.; Knebel, G.; Guber, A. E.; Heckele, M.; Herrmann, D.; Muslija, A.; Schaller, T. *Sensors Mater.* **2002**, *14*, 119−128.
(34) Vasile, M. J.; Friedrich, C. R. *Microsyst. Technol.* **1996**, *2*, 144−148.
(35) Crabtree, H. J.; Cheong, E. C.; Tilroe, D. A.; Backhouse, C. *J. Anal. Chem.* **2001**, *73*, 4079−4086.
(36) Martynova, L.; Locascio, L. E.; Gaitan, M.; Kramer, G. W.; Christensen, R. G.; MacCrehan, W. A. *Anal. Chem.* **1997**, *69*, 4783−4789.
(37) Starkey, D. E.; Han, A.; Bao, J. J.; Chong, A. H.; Wehmeyer, K. R.; Prenger, M. C.; Halsall, H. B.; Heineman, W. R. *J. Chromatogr., B* **2001**, *762*, 33−41.
(38) See Supporting Information.

electrodes (2 cm) were connected to electric cables from the high-voltage switch box and were placed in the corresponding reservoirs. For all microchips, voltages were applied to the four reservoirs for 20 (injection) and 45 s (separation). A reversed-polarity electrophoresis scheme was used in all microchips, which is similar to the common pinched injection scheme.[39] In the case that a chip needed to be reused, the channels were reconditioned by flushing with buffer. Unless otherwise stated, the following field strengths were used for all microchips: injection (481 V/cm), pullback (376 V/cm), and separation (566 V/cm). Analyte was detected 20 mm from the site of injection for all microchips. Up to eight consecutive injections and separations were done for reproducibility studies. Unless otherwise stated, the photomultiplier tube electronic sensitivity used was 50 μA with an offset of 100 nA for all microchips.

Safety Considerations. Extreme care should be used when operating high-voltage switch boxes. A built-in locking safety mechanism was used to protect the user from high voltages within the unit.

RESULTS AND DISCUSSION

Microchip Performance. It would be desirable for microchips fabricated using molding masters generated by the viable, economical, and widely accessible CNC milling to have an analytical performance similar in quality to those fabricated by more rigorous methods (e.g., LIGA, glass). Such microchips would provide not only a low-cost approach for designing and prototyping new microfluidic networks but also easier entry into microchip research for investigators without access to higher cost fabrication equipment. Because it has been previously reported that conventional CNC milling cannot be used to develop prototypes with dimensions required for microfluidic devices,[31] we sought to characterize the analytical performance of microchips fabricated using CNC-generated molding masters created by the new machining approaches we recently outlined.[25]

The analytical performance of microchips was characterized by obtaining electrophoretic data from a variety of commercial microchips and others generated in-house. PMMA microchips fabricated from CNC-generated molds used a conventional cross-injector design, in which the width and depth of the injection channel were equal to the width and depth of the separation channel. It has been noted that this design allows controlled dispensing of a discrete volume of the sample plug.[40,41] This process of loading and dispensing is fundamental to microfluidic devices and plays a critical role when samples are to be manipulated inside the microfluidic networks for mixing, chemical modifications/tagging, and analysis.

Figure 2 shows SEM images of the injector (i.e., cross) region from three different PMMA microchips replicated from three different CNC molds. The curvature seen at the junction (site of dispensing) is due to the radius of the corresponding end mill used in the fabrication of the mold. The microchip in Figure 2a, denoted hereafter as the large cross microchip, has a diagonal length of 447 μm, which is equivalent to a volume of 40 nL. The medium cross microchip, Figure 2b, has a diagonal length of 272 μm, which is equivalent to a volume of 15 nL at the dispensing site. The small cross microchip, Figure 2c, has a diagonal length of 83 μm, which is equivalent to a volume of only 1.4 nL. CNC

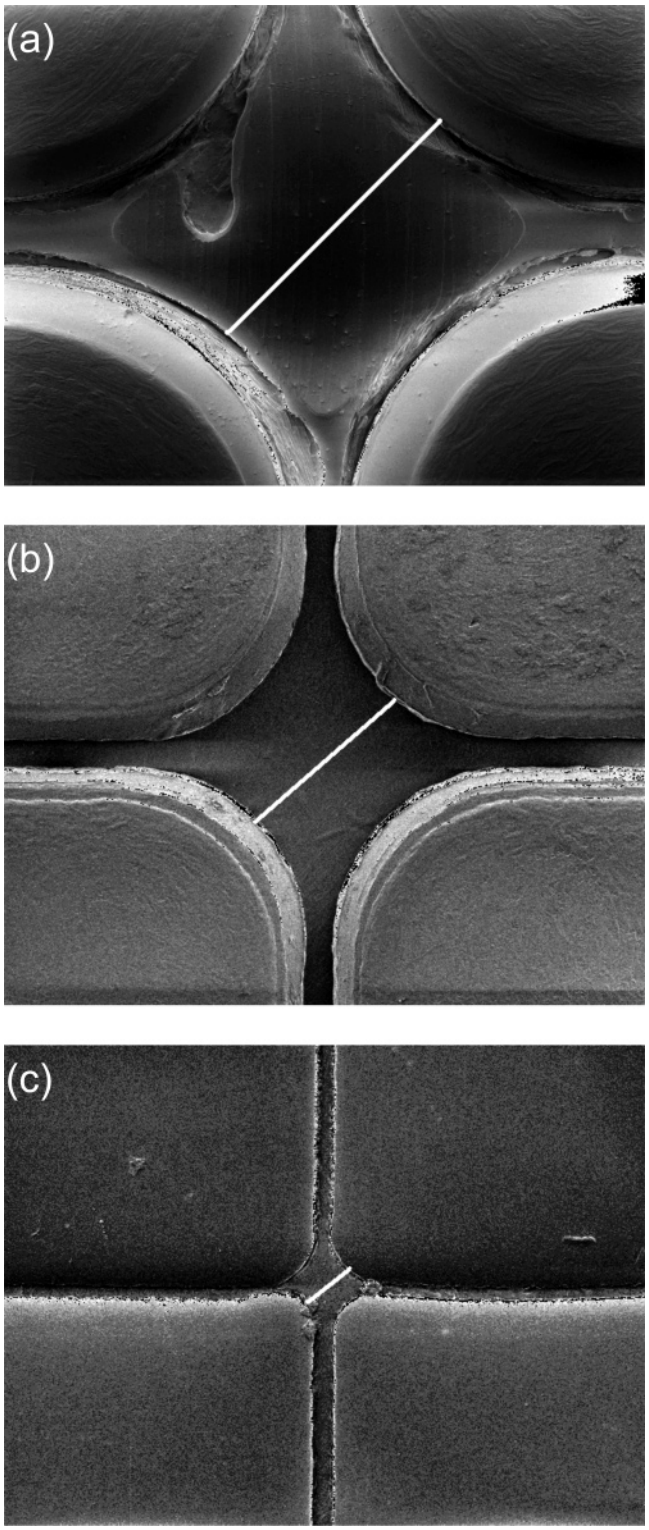

Figure 2. Scanning electron microscopy images of the cross injector (i.e., site of sample dispensing) for PMMA microchips replicated from CNC milled molding tools. All images were obtained at 130× magnification with an acquired voltage of 1 kV. (a) A large cross PMMA microchip. White diagonal bar corresponds to 447-μm diagonal distance. (b) A medium cross PMMA microchip. White diagonal bar corresponds to 272-μm distance. (c) A small cross PMMA microchip. White diagonal bar corresponds to 83-μm distance.

(39) Alarie, J. P.; Jacobson, S. C.; Ramsey, J. M. *Electrophoresis* **2001**, *22*, 312−317.
(40) Bousse, L.; Cohen, C.; Nikiforov, T.; Chow, A.; Kopf-Sill, A. R.; Dubrow, R.; Parce, W. J. *Annu. Rev. Biophys. Biomed. Struct.* **2000**, *29*, 155−181.
(41) Li, D. Electrokinetics in Microfluidics; Elsevier: Boston. 2004.

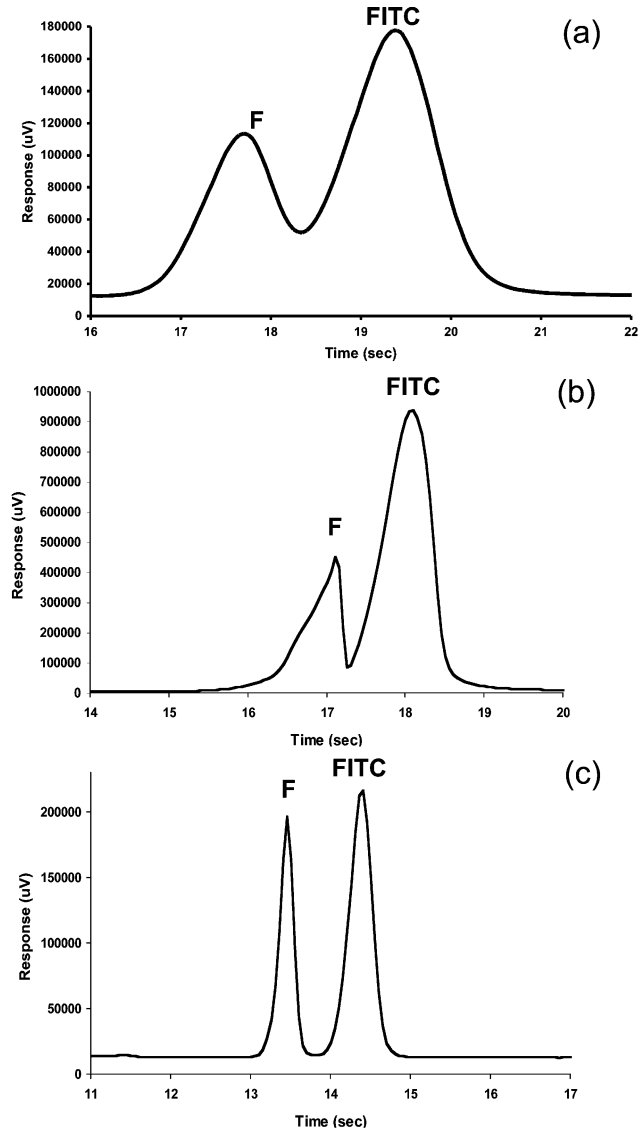

Figure 3. Electropherograms of fluorescein (F) and fluorescein isothiocyanate (FITC) obtained under the following experimental conditions. An electric field strength of 481 V/cm was applied between the sample waste and sample injection reservoirs for 20 s, and then a separation field strength of 566 V/cm was applied between the buffer waste and buffer reservoirs, with pull back field strengths of 376 V/cm to sample injection and sample waste reservoirs, respectively, for 45 s. Electropherograms obtained with (a) large cross, (b) medium cross, and (c) small cross CNC microchips. All other conditions are given in Materials and Methods.

mold fabrication time and effort are inversely proportional to the size of the cutting tool, and so smaller junction volumes require considerably more time, expense, and effort to fabricate. Goals of this work were to determine the largest junction sizes (i.e., least costly fabrication choice) that still yield an analytical performance acceptable for prototyping and to find junction sizes whose performance is comparable to that available from commercial microchips. We evaluated analytical performance using on-chip electrophoresis.

Electropherograms for separating fluorescein and FITC in the three microchips replicated from various CNC molds are shown in Figure 3. Similar studies were also done using glass, commercial PMMA, LIGA, and wire-imprinted microchips for comparison (Figure 4), with the relevant analytical figures of merit for all microchips investigated provided in Tables 1 and S1.[38] As

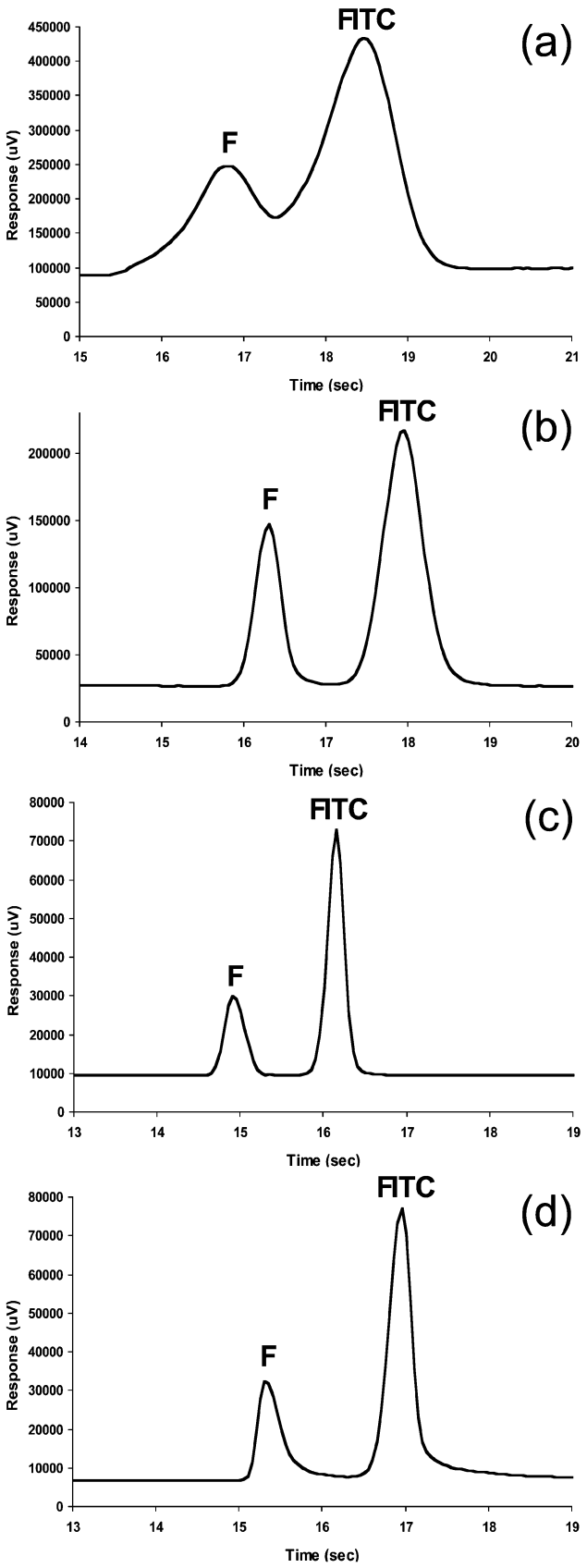

Figure 4. Electropherograms of fluorescein (F) and fluorescein isothiocyanate (FITC) obtained under the same experimental conditions as in Figure 3 from the following microchips: (a) wire-imprinted, (b) commercial PMMA (Aclara), (c) LIGA, and (d) commercial glass.

Table 1. Analytical Performance of Various Microchips Investigated in This Work[a]

microchip[b]	T_m[c]	P_a[c]	$W_{1/2}$[c]	W_b[c]	N[c]	R[d]
small cross	13.70 ± 0.22	3.8 ± 0.1 (x10^4)	0.24 ± 0.01	0.47 ± 0.06	19 ± 0.1	1.97 ± 0.08
medium cross[e]	17.09 ± 0.07	2.3 ± 0.1 (x10^5)	0.41 ± 0.01	0.81 ± 0.03	9.6 ± 0.3	1.02 ± 0.07
large cross	16.83 ± 1.22	7.9 ± 3.6 (x10^4)	0.88 ± 0.18	1.78 ± 0.38	2.2 ± 0.7	0.86 ± 0.12
LIGA	15.05 ± 0.07	5.9 ± 0.2 (x10^3)	0.24 ± 0.00	0.49 ± 0.00	21 ± 0.3	2.76 ± 0.02
Glass	14.98 ± 0.35	7.8 ± 0.1 (x10^3)	0.24 ± 0.01	0.50 ± 0.03	22 ± 0.4	2.93± 0.06
ACLARA	16.42 ± 0.09	4.6 ± 0.1 (x10^4)	0.36 ± 0.01	0.72 ± 0.02	11 ± 0.4	1.85 ± 0.03
Wire Imprinting	16.99 ± 0.14	1.7 ± 0.1 (x10^5)	0.86 ± 0.01	1.77 ± 0.07	2.2 ± 0.1	0.91 ± 0.02

[a] A sample of fluorescein (F) and fluorescein isothiocyanate (FITC) was analyzed using fluorescence detection for 65 s/injection. The values reported in the table are the averages of four injections. [b] Unless stated, the data for various microchips were obtained under the conditions for Figures 3 and 4. [c] The migration time (T_m) (in s), peak area (P_a) (μV·s), width at half-peak ($W_{1/2}$) (in s), width at baseline (W_b) (in s), and number of theoretical plates (N) (×1000) were for fluorescein. [d] R was the resolution between FITC and fluorescein. Standard deviations were calculated for runs 2−5. [e] Results generated at 100 μA sensitivity.

expected, peak widths at half-height, and baselines, increased in proportion to increases in junction size, and the resolution and number of theoretical plates decreased with increasing junction size for microchips replicated from the CNC molds.

Large Cross Microchip. The analytical performance of the large cross microchip, which was the easiest to fabricate (design-to-device time ~4 h), was clearly the poorest of the three, providing a performance most similar to the microchip fabricated by wire imprinting. As can be seen in Figures 3a and 4a, fluorescein and FITC are not well separated. While peak areas were larger for the wire-imprinted chip, migration times, resolution, and theoretical plate number were nearly identical for the two microchips. However, a larger standard deviation in the performance data was noted in the large cross microchip, which was attributed to some diffusion of analyte into the site of injection.

Medium Cross Microchip. Fabricating the mold used to replicate the medium cross microchips was slightly more time-consuming than the fabrication required for the large cross mold (~1 additional hour). From a performance perspective, the additional effort required in the mold fabrication is worthwhile, because these microchips are comparable in performance to the commercial PMMA microchip. In contrast to the CNC chip, the commercial PMMA microchip has an offset T (250 μm) design, which provides a more defined sample plug compared to the medium cross design used in this study. As can be seen in Figures 3b and 4b, fluorescein and FITC are well separated on both microchips. A slightly greater separation efficiency was obtained from the commercial microchip than the medium cross microchip, although the differences in peak widths were not significant (0.72 (commercial microchip peak width) vs 0.81 s (medium cross microchip peak width)). The column efficiencies, as determined by the number of theoretical plates, were similar on both platforms (1.1×10^4 (commercial microchip) versus 9.6×10^3 (medium cross microchip)).

The decreased resolution obtained in the medium cross microchip may be ascribed to a larger plug size as well as potential leakage at the junction. Leakage and plug size have been shown to affect column efficiency using various injector geometries.[42] However, slightly larger peak areas were obtained from the medium cross microchip than the commercial microchip. Overall, the medium cross microchip provides an analytical performance comparable to that from a commercial microchip, demonstrating that microchips replicated from CNC molding masters are suitable for analytical-scale microchip studies.

Small Cross Microchip. The CNC mold used to replicate the small cross microchips requires substantially longer machining times (total of ~9−10 h) than either of the other two CNC molds. These microchips represent the limit one can reasonably obtain in channel dimensions and junction sizes from commercial CNC milling devices. An evaluation of the data from Table 1 finds that the small cross microchip provides analytical figures of merit most comparable to commercial glass microchips and microchips replicated from LIGA molds. Unlike the curvature seen at the junctions in CNC microchips, LIGA molds have well-defined right angles at these junctions. Fluorescein and FITC were well separated (Figures 3c and 4c), while migration times for fluorescein were slightly less (~1.3 s) on the small cross microchip than on the LIGA microchip. Not surprisingly, the theoretical plate number was ~2000 plates higher for the LIGA microchip than for the CNC microchip. The substantially higher sensitivity obtained from the small cross microchip, in comparison to the LIGA microchip, can be attributed to the larger plug size injected using the CNC device. While peak widths at half-height and baseline were comparable in both microchips, the resolution between fluorescein and FITC was greater for the LIGA microchip than the small cross microchip (2.76 vs 1.97).

The well-defined geometrical shapes at junctions in glass devices are similar to those found in the chip produced from a LIGA mold. However, glass devices have semicircle channels arising from the etching process, whereas microchips generated from LIGA or CNC milling have square features. As with the LIGA microchips, commercial glass microchips yielded a larger number of theoretical plates and higher resolution between fluorescein and FITC than the small cross microchip (Figures 3c and 4d). The carefully controlled geometrical dimensions available from commercial glass microchips and LIGA microchips result in the best analytical performance. While the small cross microchip was comparable to these other two microchips, the gain in performance between the medium and small cross microchips comes at a significant expense in machining time and effort.

Compensation for CNC Milled Junction Volume through Pullback Voltages. Machining capabilities, tolerances, and end mill dimensions ultimately determine the injection volume one can readily obtain using microchips replicated from CNC molding tools. Furthermore, as demonstrated above, moderate machining

(42) Zhang, C. X.; Manz, A. *Anal. Chem.* **2001**, *73*, 2656−2662.

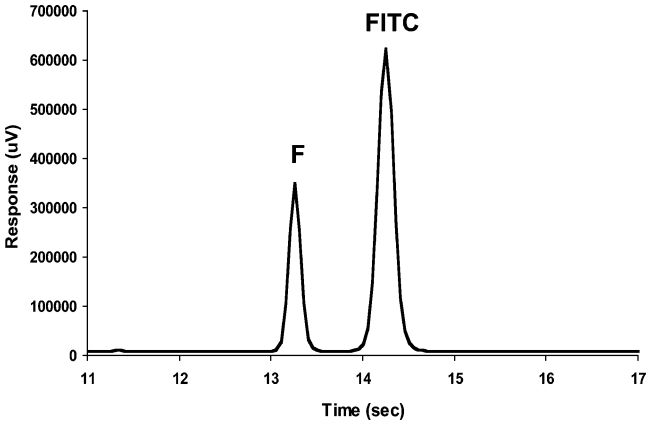

Figure 5. Electropherogram of fluorescein (F) and fluorescein isothiocyanate (FITC) obtained with the small cross CNC chip under the following experimental conditions. An electric field strength of 481 V/cm was applied between the sample waste and sample injection reservoirs for 20 s, and then a separation field strength of 566 V/cm was applied between the buffer waste and buffer reservoirs, with pull back field strengths of 479 V/cm to sample injection and sample waste reservoirs, respectively, for 45 s. All other conditions are given in Materials and Methods.

efforts can yield molds suitable for prototyping or even routine analytical use. However, in an effort to further improve the separation performance of microchips made from CNC molding tools, higher pullback field strengths were investigated. A comparison of the significance of the pullback voltage field strength on chip performance was made using a small cross CNC chip and the LIGA chip.

In the case of the LIGA chip, a higher pullback field strength (479 V/cm) was applied during the separation step than in the previously mentioned experiments. Only moderate increases (22×10^3 vs 26×10^3) in plate counts were evident. Resolution remained the same, and the migration times experienced a marginal decrease of ~0.7 s.[38] The peak area and peak height increase seen with the LIGA devices at these higher pullback field strengths have been theoretically described previously.[41] These moderate improvements in performance can be attributed to the already well-defined junction in the devices fabricated from LIGA molds.

The electropherogram shown in Figure 5 was obtained with the CNC chip using the same increased pullback field strength as used for the LIGA chip. At the higher pullback field strength, a 2-fold increase (19×10^3 vs 42×10^3) in plate number (column efficiency) was noted. Resolution increased from 2.00 to 3.12, and shorter migration times (~0.25 s) were also evident.[38] Interestingly, an increase in sensitivity and peak areas was also seen when higher pullback voltages were applied. Thus, the larger, less well-defined junction volumes inherent to the CNC devices may be compensated for by the judicious application of pullback voltages to yield extremely reasonable analytical performance. While the current investigations used fluorescence detection, other detection methods should also be compatible with microchips made from CNC molding tools. These methods, and assay developments for analytical applications using such microchips, are currently being investigated in our laboratories.

CONCLUSIONS

We have shown that thermoplastic microchips fabricated using CNC-generated molding masters yield an analytical performance related to the channel dimensions and injector volume as would be expected. However, these studies reveal that microchips can be fabricated from CNC-generated molding masters to yield analytical performance at levels comparable to those found from commercially available devices, which contrasts with previous comments on their applicability.[31] The advantages of the outlined fabrication process arise from the wide availability and relatively low cost of CNC machining devices in commercial and academic settings. With no additional investment in machining equipment, researchers have a new entry point for initiating research and development studies using thermoplastic microfluidic devices. While our data demonstrate that high-performance microchips are attainable by this process, the more likely use will arise in prototyping and one-off master mold generation. Production-level generation of microchips would not be recommended from this approach. Although microchips fabricated in this fashion are appropriate for analytical use, there are several limitations. In particular, the CNC milling technique for mold generation would be deemed inferior when a design is needed for channels to be closer than the radius of the end mill tool, which in this case was 51 μm, or if the channel widths were required to be less than 25 μm in width. It would be more appropriate and effective to migrate to micromachining equipment when these smaller dimensions are required in the molding tool.

ACKNOWLEDGMENT

Financial support of this work was provided by the National Science Foundation (DBI-0137924), the National Institutes of Health (GM 69547), and the University of Cincinnati. The authors also thank Drs. S. Conklin, B. Berhane, and D. Starkey for their assistance at various stages of this project.

SUPPORTING INFORMATION AVAILABLE

Additional figures of merit. This material is available free of charge via the Internet at http://pubs.acs.org.

Received for Review August 25, 2005. Accepted November 24, 2005.

AC051523Y